Changes of Coupling between the Electrodes and the Molecule under External Bias Bring Negative Differential Resistance

Xingqiang Shi, Xiaohong Zheng, Zhenxiang Dai, Yang Wang, and Zhi Zeng*

Key Laboratory of Materials Physics, Institute of Solid State Physics, Chinese Academy of Sciences and Graduate School of the Chinese Academy of Sciences, Hefei 230031, P.R. China

We report a first-principles study of electrical transport and negative differential resistance (NDR) in a single molecular conductor consisting of a borazine ring sandwiched between two Au(100) electrodes with a finite cross section. The projected density of states (PDOS) and transmission coefficients under various external voltage biases are analyzed, and it suggests that the variation of the coupling between the molecule and the electrodes with external bias leads to NDR. Therefore, we propose that one origin of NDR in molecular devices is caused by the characteristics of both the molecule and the electrodes as well as their cooperation, not necessarily only by the inherent properties of certain species of molecules themselves. The changes of charge state of the molecule have minor effects on NDR in this device because the Mulliken population analysis shows that electron occupation variation on the molecule is very small when different external biases are applied.

I. Introduction

An important goal in molecular electronics is to use molecular devices to realize the elementary functions in electronic circuits,[1] such as storage, rectification, and amplification. Negative differential resistance (NDR) phenomenon in molecular conductors, which is characterized by a decreasing current through the junction at an increasing voltage bias, has gained widespread interest from molecular electronics researchers because NDR is the basic principle of several electronic components, such as the Esaki diode and resonant tunneling diode,[2,3] and the resonant tunneling diode can be used as the basis of memory, switching, and logic functionality.[3]

Thus far NDR effects have already been observed from a large number of measurements with different methods in different molecules, and different details of the current–voltage characteristics have been discovered.[4–14] However, the corresponding physical mechanisms governing the NDR effects in most of this experimental work are seldom mentioned. A lot of theoretical work on NDR has also been performed,[15–19] and several mechanisms based on charge transfer and conformational change have been proposed.[15–18] In particular, Seminario et al. studied the electronic structure and geometry structure of the isolated phenyl-ethynylene oligomers (OPEs) and tried to explain the NDR mechanism found experimentally in OPEs by Reed and co-workers.[4] They proposed that NDR in these molecules is caused by the change of the electronic charge state of the molecule under increasing biases and the subsequent change of the molecular conformation due to the change of the charge state.[15] When the molecules are singly reduced, the lowest unoccupied molecular orbital (LUMO) is quite delocalized and electrons can transmit through it easily. When the molecules are neutral or doubly reduced, the LUMO is very local and the electron transmission will be blocked. However, calculations done by Stokbro et al. on OPEs which are connected

by two electrodes show that the NDR is related to rotations of the middle phenyl ring of the molecules but charging effects are not important.[19] NDR effects have also been obtained theoretically in atomic wires[20] and clusters.[21] These studies suggest that NDR cannot be associated only with the molecule studied, but the role of the electrodes must also be taken into consideration. Obviously, despite much experimental and theoretical research on NDR, the physical picture governing the NDR effects in molecular devices has not been well understood, and further theoretical investigation is still necessary.

A popular model system to understand the electrical transport properties of the metal–molecule–metal system is the benzene molecule.[22–24] Borazine is isoelectronic with benzene and shows a larger energy gap between the highest occupied molecular orbital (HOMO) and the lowest unoccupied molecular orbital (LUMO) than the benzene ring does.[25] More interestingly, NDR has been reported in the borazine ring in Bai's theoretical research,[26] while the mechanism governing NDR in it is not yet clearly clarified.

To contribute to the knowledge about the mechanism of NDR in single molecular devices, in the current research we present a detailed first-principles analysis of the $I-V$ characteristics of the borazine ring sandwiched between two Au(100) electrodes with a finite cross section. Our results suggest that NDR is mainly attributed to the changes of the coupling between the molecular orbitals in the borazine and the incident states of the electrodes under external bias and is not caused by the changes of the charge state of the molecule since the electron occupation variation on the molecule is very small when different external biases are applied.

This paper is organized as follows: In section II we give a brief description of the calculation method (the TranSIESTA-C package[27–29]) and the simulation model. Section III presents calculations of the $I-V$ curve of the thiolate-bonded borazine molecule together with an analysis of the projected density of states (PDOS) and Mulliken population which are important

* To whom correspondence should be addressed. E-mail: zzeng@theory.issp.ac.cn.
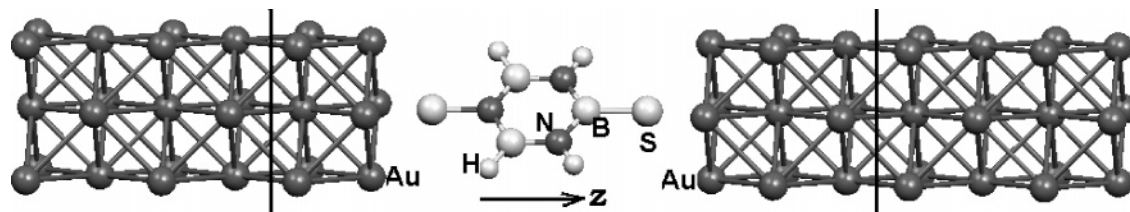
Changes of Coupling

J. Phys. Chem. B, Vol. 109, No. 8, 2005 **3335**

Figure 1. Computational cell used for determining the $I-V$ characteristics of dithiolborazine coupled to Au(100) electrodes with a finite cross section (we chose a supercell with a large enough vacuum layer around the electrode in the x and y directions so that the device has no interaction with its mirror images). The region within two black lines is the scattering region, and the remaining parts are the left and right electrodes. The gold electrodes extend to $z = \pm\infty$.

for analysis of electron transmission. A short summary is given in section IV.

II. Calculation Method and Simulation Model

The TranSIESTA-C package is used in this work to study the transport properties of a two-probe system. TranSIESTA-C combines the well-tested electronic structure calculation method SIESTA[29] and the NEGF (nonequilibrium green function) technique[30,31] to simulate electrical transport in molecular devices under a nonequilibrium situation. The principles and technique details of this method can be found in the listed references.[27,28,32]

A two-probe molecular device consists of three parts: the left electrode, the scattering region, and the right electrode. Figure 1 shows the studied system model: A dithiolborazine molecule sandwiched between two Au(100) contacts. The dithiolborazine molecule together with two layers of the surface atoms in the left and three layers of surface atoms in the right that interact with the molecule are chosen as the scattering region. The remaining parts are the left and right electrodes (see Figure 1). The sulfur atoms, adopted as the alligator clips to provide chemical and geometrical stability between the molecule and Au electrodes, are positioned symmetrically above the Au-(100) hollow sites. The molecular geometry is obtained by primarily optimizing the geometry of the free molecule with H atoms attached to the sulfur atoms. Then, we place the molecule between the electrodes with an initial Au−S distance of 2.1 Å[33] and relax the extended molecule (dithiolborazine + four layers of gold atoms in each electrode) to determine the final Au−S distance and equilibrium dithiolborazine coordinates by DMol.[34] Since the Au basis[35] range (3.5 Å) only extends to the two neighboring gold electrode layers, we take four gold layers for the electrode unit cell to ensure that only atoms in the nearest-neighbor electrode cells in the z direction have interactions, which is a requirement of the TranSIESTA-C package in choosing the electrode cells. Thus, an electrode unit cell consists of 18 Au atoms.

The system subjected to an external bias is highly in nonequilibrium. The left- and right-moving carriers have significantly different chemical potentials, and the electrostatic potential is a function of position in the molecule. Therefore, a full self-consistency method to describe it is necessary. In the TranSIESTA-C code a full self-consistency procedure of the electronic structure of the scattering region is performed before the transmission function and the current are calculated under each bias voltage. The electronic structure of the two electrodes is calculated only once before the self-consistency procedure of the scattering region starts, and the self-consistent potential in the electrodes will be shifted rigidly relative to each other by the external voltage biases.[23] A SIESTA localized basis set is used to expand the valance electron wave functions, and the core electrons are modeled by standard nonlocal norm conserv-
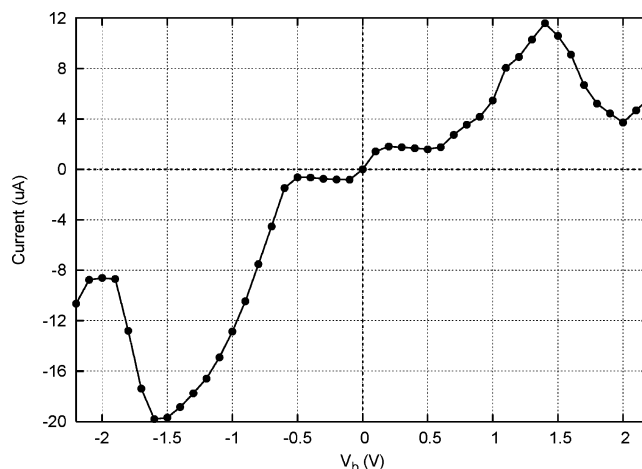

Figure 2. Current of the open system as a function of external voltage biases.

ing pseudopotential.[36] To calculate the electrostatic potential distribution (Kohn−Sham potential) in the scattering region, the electron density is required, and it is calculated by the density matrix which is constructed via NEGF technique. The potential in the semi-infinite electrodes provides natural real space boundary conditions for the Kohn−Sham potential of the scattering region. The coupling of the scattering region with the electrodes is taken into account by self-energies. The Kohn−Sham potential includes contributions from Hartree, exchange, correlation, the atomic core, and any other external potentials. The procedure is iterated until the convergence criterion 10^{-4} is achieved for both the Hamiltonian and the charge density.

We calculate transport properties within the coherent transport regime. Two other effects, i.e., electronic correlations[37,38] and molecular vibrational modes, which might be important for transport, are neglected in the current work.

III. Results and Discussions

Figure 2 shows the $I-V$ curve of the system. The $I-V$ curve is not quantitatively equal in the positive and negative bias parts due to the unsymmetrical electronic structure of dithiolborazine along the z direction and the corresponding unsymmetrical coupling to the left and right electrodes. However, the two parts of the $I-V$ curve with positive and negative bias are qualitatively similar, namely, they both exemplify NDR behavior. In particular, we only focus on the positive bias part of the $I-V$ curve. We will show that the appearance of a platform in 0.2−0.6 V and NDR in 1.4−2.0 V in the $I-V$ characteristics can be understood by studying the changes of coupling between the molecular orbitals in the dithiolborazine and incident states in the electrodes under various external biases.

Figure 3 shows the zero bias transmission spectra of the system and the projected density of states (PDOS) of the molecule. In the zero bias transmission spectra, there are two
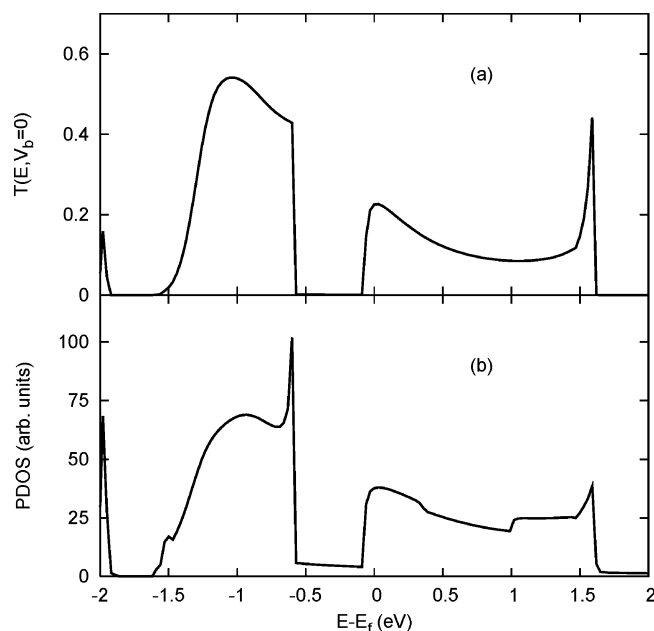
Figure 3. (a) Transmission coefficients under zero bias as a function of energy. (b) The corresponding PDOS. All energy is relative to the Fermi energy of the open system.

energy regions, $[-1.6,-0.6]$ and $[-0.1,1.6]$, where electrons incident from one of the electrodes can transmit across the molecule to the other electrode significantly. We refer to these two energy regions as "significant energy regions" (SERs) because incident electrons in these regions contribute most significantly to the transmission spectra. It is important to emphasize that the SERs in the electrodes are determined by the characteristics of both the molecule and the electrodes. Different molecules sandwiched between the same electrodes may give different SERs. To understand why incident states in these two energy regions can transmit across the molecule significantly, we calculated the projection of the density of states of the combined system onto all the dithiolborazine basis orbitals (PDOS). The PDOS is calculated by

$$P(E) = \langle \psi^m(E) | \Psi(E) \rangle$$

$$= \langle \sum_i^{mol.} c_i(E)\phi_i(\vec{r}) | \sum_j^{all} c_j(E)\phi_j(\vec{r}) \rangle,$$

where $\Psi(E)$ is the eigenstate of the whole system and $\psi^m(E)$ is the contribution of the basis orbitals of the molecule to $\Psi(E)$, $\{\phi\}$ are the nonorthogonal basis set of the system, and c_i and c_j are expanding coefficients. The sum over i only runs over the basis orbitals of the molecule, and the sum over j runs over all the basis orbitals of the whole system. The PDOS will give us information on how much the basis orbitals in the molecule contribute to the eigenstate of the whole open system and how strongly the molecule couples with the electrodes at a certain energy E. The PDOS is shown in Figure 3b. We note that, corresponding to the $T-E$ curve, there are also two energy regions $[-1.6,-0.6]$ and $[-0.1,1.6]$ where the PDOS takes a comparatively large value. A strong coupling makes incident electrons at a certain energy easily transmit across the molecule, and this will give rise to a large transmission coefficient at this energy. This is clearly shown by comparison of the transmission spectra and PDOS spectra shown in Figure 3a and b. As a consequence, a large transmission coefficient indicates a strong coupling between the electrodes and the molecule, and the

evolution of transmission curves with external biases can help us understand how the changes of the coupling between the electrodes and molecule determines the $I-V$ characteristics in the system. Therefore, the voltage dependence of the transmission function will be studied next.

Now we divide the whole energy region into two kinds of regions according to whether $T(E, V_b) = 0$ or not in them. In the regions where $T(E, V_b)$ is not zero the incident electrons can transmit across the molecule, and we call them transmission regions. In the other regions where $T(E, V_b)$ is zero the incident electrons cannot transmit across the molecule, and we call them transmission intervals.

The current in the system is calculated by the Landauer–Büttiker formula $I = (2e/h)\int T(E, V_b)dE$, which is transmission spectra dependent. We will now show the changes of the transmission function under various biases in a three-dimensional plot (Figure 4). We see that the transmission interval near the Fermi energy under zero bias is broadened and doubled at increasing biases. It can be explained by the relative shift of the SERs of the left and right electrodes. Figure 5 illustrates how the SERs in the left and right electrodes are shifted under external biases.

Figure 5a shows the SERs in the left and right electrodes (denoted by light gray boxes) and the transmission regions (dark gray boxes) at zero bias. When external bias is applied the electrochemical potential in the left/right electrode ($\mu_L(V_b)$, $\mu_R(V_b)$) will be shifted. For instance, when $V_b = 1 (V)$, $eV_b = \mu_L(V_b) - \mu_R(V_b) = -1$ (eV), where $\mu_L(V_b) = E_f + eV_b/2$ and $\mu_R(V_b) = E_f - eV_b/2$. When the external bias is 0.2 V, the SER is shifted by -0.1 eV in the left electrode and 0.1 eV in the right electrode (see Figure 5b). The displacement of SERs in the left/right electrode reduces the transmission regions from $[-1.6,-0.6]$ and $[-0.1,1.6]$ to $[-1.5,-0.7]$ and $[0.0,1.5]$ and the transmission interval is broadened from $[-0.6,-0.1]$ to $[-0.7,0.0]$, respectively (see Figures 5b and 4). At 0.6 V, due to the further displacement of SERs in the left/right electrode, except for further reduction of the transmission regions, a new transmission region $[-0.4,-0.3]$ arises in the original zero bias transmission interval (see Figure 5c). This is because the bottom part of the higher SER of the left electrode now aligns with the top part of the lower SER of the right electrode. In later discussions we will see that the $I-V$ characteristics above 0.6 V are mainly determined by the changes of this new transmission region under various biases. With similar analysis of the displacement of SERs in the left and right electrodes under various external bias we can understand why the transmission curves evolve in the way plotted in Figure 4.

Now let us see why the current curve is like this: a platform in 0.2–0.6 V, a rise in 0.6–1.4 V, and NDR in 1.4–2.0 V. The current, I, is obtained from $I = (2e/h)\int_{\mu L}^{\mu R} T(E, V_b)dE$, where $\mu_L(V_b)/\mu_R(V_b)$ are the electrochemical potentials of the left/right electrodes. The region between μ_L and μ_R is called the bias window or integral window, as shown in Figure 4 with the dashed lines and Figure 5 with black boxes, respectively. Thus, the current is determined by $T(E, V_b)$ in the bias window and is further only determined by the transmission regions in the bias window because $T(E, V_b)$ is zero in the transmission interval and has no contribution to the current. It can be seen from Figure 4 or Figure 5b and c that with the external bias increasing from 0.2 to 0.6 V, no additional transmission region will be included into the bias window, though the bias window at 0.6 V is much larger than that at 0.2 V. As a result, the current, I, will not increase from 0.2 to 0.6 V. Thus, a platform appears in this voltage range. As the external bias further increases, the

Changes of Coupling

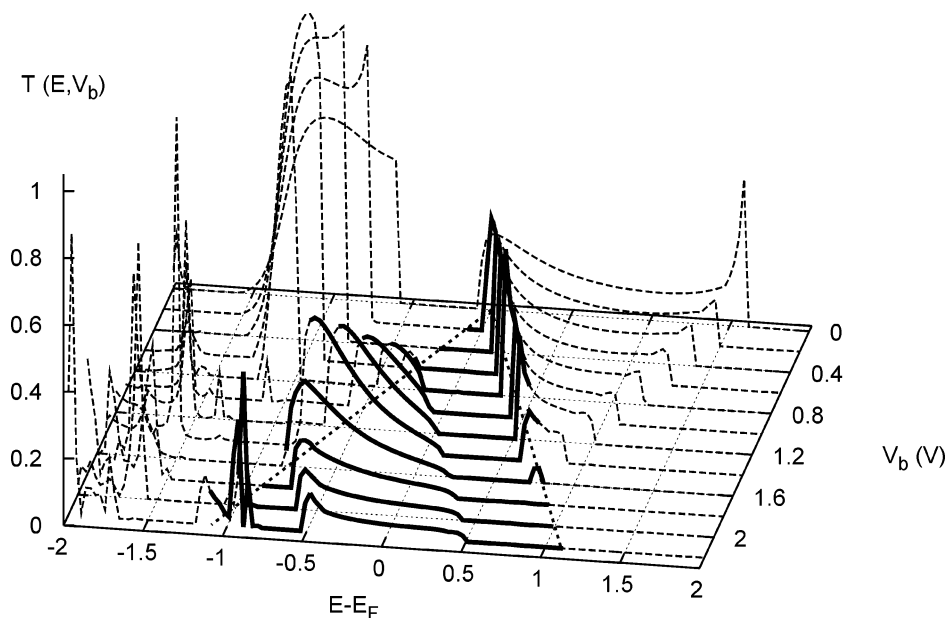*J. Phys. Chem. B, Vol. 109, No. 8, 2005* **3337**

Figure 4. Three-dimensional plot of the bias dependence of the transmission spectra. Regions between the dashed lines are the bias window, and the transmission curves in these regions are shown with thick solid lines. Energy is relative to the Fermi energy of the open system.
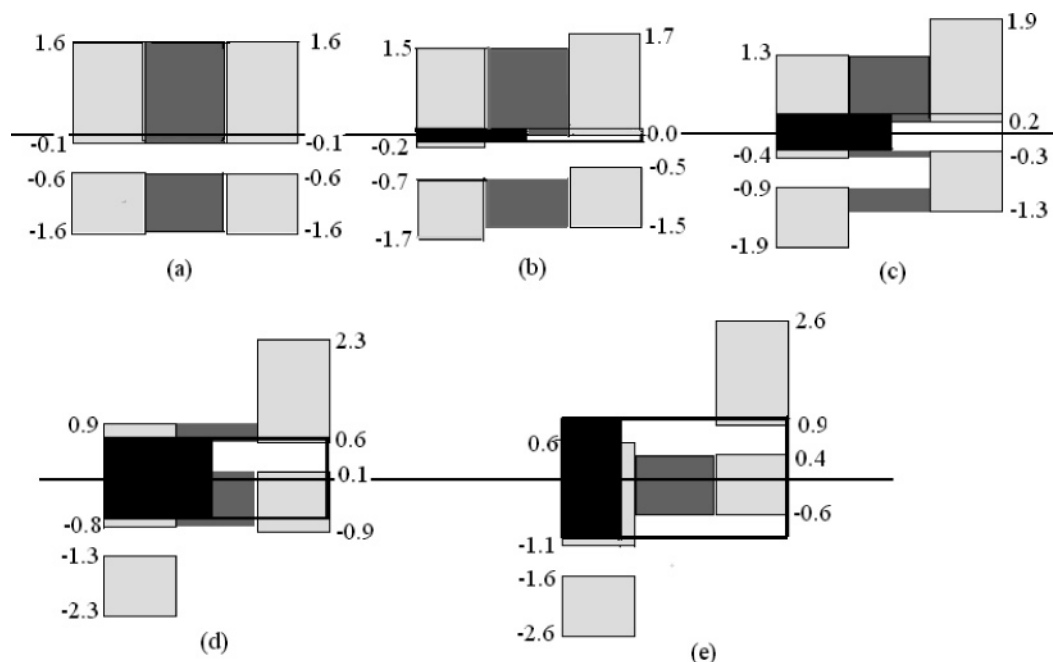

Figure 5. Displacement of SERs in the left and right electrodes and transmission regions under various external bias: (a) 0, (b) 0.2, (c) 0.6, (d) 1.4, and (e) 2.0 V. (Light gray boxes) SERs in the left and right electrodes. (Dark gray boxes) Transmission regions. (Black boxes) The bias window. To show the dark gray boxes, the black boxes are half filled. All energy values are in eV and relative to the Fermi energy. (Black solid line) Fermi level of the whole open system.

new transmission region broadens rapidly since the electrons in the higher SER of the left electrode can transmit across the molecule to the lower SER of the right electrode in an increasingly wider energy region. As a result, the current increases quickly until 1.4 V. After 1.4 V the whole range of the lower SER in the right electrode overlaps with part of the higher SER in the left electrode. This can be seen in Figure 5e, and it can also be clearly identified in Figure 4. Figure 4 shows that the width of the new transmission regions in the bias window always remains unchanged after 1.4 V, although it moves to the right with increasing bias. Another important point to note is that the transmission coefficients in the new transmission region are getting smaller and smaller. This is why the current in voltage range 1.4−2.0 V decreases rapidly, and

NDR appears in this voltage range. From the earlier discussion we know that a smaller transmission coefficient indicates a weaker coupling between the molecular orbitals in the dithiol-borazine and the incident states from the electrodes. Thus, NDR appears as a combination of two facts that the coupling of the molecular orbitals in the dithiolborazine to the incident states from the electrodes decreases[39] and the transmission regions in the bias window does not get wider with increasing biases. We are aware that in Figure 5 we only focus on the two SERs nearest the Fermi level since other energy regions that have a contribution to the transmission coefficients are out of the bias window with an external voltage of less than 2.0 V. After 2.0 V other transmission regions enter the bias window significantly and the current increases again.
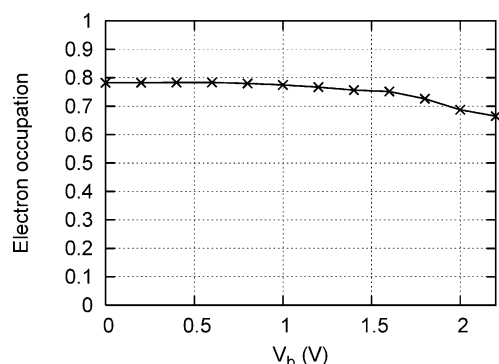
Figure 6. Net charge on the molecule as a function of bias.

Theoretical studies by Seminario et al., based on studies of isolated molecules, propose that the molecules change their charge state when external bias is applied and that this leads to NDR.[15,16] In the present work we deal with an open metal−molecule−metal system and the charge on the molecule is not fixed when external voltage bias is changed. From a Mulliken population analysis we obtain the net charge on the molecule under various biases (see Figure 6). We find that there is a noticeable charge transfer (about 0.78 e) from the electrodes to the molecule at equilibrium (zero bias). This acts not only to align the Fermi level of the molecule and the electrodes, but also to build up a Schotky-barrier-like structure through the formation of an interface dipole.[24] Note that only slightly additional charge is drawn out of the molecule after external bias is applied, as shown in Figure 6 (less than 0.1 e in 0.0−2.0 V). Thus, our calculations indicate that charging effects on NDR in this device are not important. This is in agreement with theoretical studies of reference.[19]

IV. Conclusion

In conclusion, we studied the $I−V$ characteristics and NDR in dithiolborazine coupled to Au(100) electrodes with a finite cross section. Our study shows that the NDR in this device is determined by displacement of the SERs under various external biases. There is no direct relation between NDR and the charge state of the molecule because the additional electron transfer between the molecule and the electrodes is negligible after various biases are applied.

The SERs describe the coupling of the incident states in the electrodes and the molecular orbitals in the functional molecule and are determined by features of both the molecule and the electrodes. Thus, a molecule may display different transport behaviors in different situations, for instance, with a different selection of electrodes. Our further study shows that dithiol-benzene sandwiched between Au(100) electrodes with a finite cross section also displays NDR behavior. All these remind us that in the design of molecular devices the information of the electrodes must also be taken into consideration very seriously.

In this work the choice of electrodes with a finite cross section might be somehow artificial. However, our starting point is to model a nanowire electrode. Generally, the atomic structure of a nanowire cannot easily be known, so we choose such an artificial model, which is often chosen this way by others (see, for example, refs 20,40, and 41). It is important to clarify whether NDR is mainly from the molecule or mainly from the electrodes. In the system studied here NDR is mainly derived from the functional molecule. There are at least two relevant theoretical studies to support this point of view. The first one is by Guo and co-workers,[40] who used the same electrodes but chose silicon clusters as the molecule, and no NDR appears

there. The second one is Bai et al.,[7] who chose a more realistic electrode with a Au(111) surface structure for the same molecule, and they also got the NDR. However, the $I−V$ characteristics there are not quite the same and the peak-to-valley ratio of the current is much smaller than that in the present work. This might be due to the different band structures of the electrodes and the different couplings between the molecule and electrodes. Therefore, electrodes with finite cross sections may be more beneficial for the occurrence of NDR, which is also suggested by Guo et al.[20] However, this may present a challenge for experimentalists.

References and Notes

(1) Joachim, C.; Gimzewski, J. K.; Aviram, A. *Nature* **2000**, *408*, 541.
(2) Sze, S. M. Physics of Semiconductor Devices, 2nd ed.; John Wiley and Sons: New York, 1981.
(3) Mathews, R. H.; Sage, J. P.; Sollner, T. C. L. G.; Calawa, S. D.; Chen, C.-L.; Mahoney, L. J.; Maki, P. A.; Molvar, K. M. *Proc. IEEE* **1999**, *87*, 596−605.
(4) Chen, J.; Reed, M. A.; Rawlett, A. M.; Tour, J. M. *Science* **1999**, *286*, 1550.
(5) Chen, J.; Wang, W.; Reed, M. A.; Rawlett, A. M.; Price, D. W.; Tour, J. M. *Appl. Phys. Lett.* **2000**, *77*, 1224.
(6) Xue, Y.; Datta, S.; Hong, S.; Reifenberger, R.; Henderson, J. I.; Kubiak, C. P. *Phys. Rev. B* **1999**, *59*, R7852.
(7) Gorman, C. B.; Carroll, R. L.; Fuierer, R. R. *Langmuir* **2001**, *17*, 6923.
(8) Fan, F. F.; Yang, J.; Cai, L.; Price, D. W., Jr.; Dirk, S. M.; Kosynkin, D. V.; Yao, Y.; Rawlett, A. M.; Tour, J. M.; Bard, A. J. *J. Am. Chem. Soc.* **2002**, *124*, 5550.
(9) Kratochvilov, I.; Kocirik, M.; Zambova, A.; Mbindyo, J.; Mallouk, T. E.; Mayer, T. S. *J. Mater. Chem.* **2002**, *12*, 2927.
(10) Amlani, I.; Rawlett, A. M.; Nagahara, L. A.; Tsui, R. K. *Appl. Phys. Lett.* **2002**, *80*, 2761.
(11) Rawlett, A. M.; Hopson, T. J.; Nagahara, L. A.; Tsui, R. K.; Ramachandran, G. K.; Lindsay, S. M. *Appl. Phys. Lett.* **2002**, *81*, 3043.
(12) Rawlett, A. M.; Hopson, T. J.; Amlani, I.; Zhang, R.; Tresek, J.; Nagahara, L.; Tsui, R. K.; Goronkin, H. *Nanotechnology* **2003**, *14*, 377.
(13) Le, J. D.; He, Y.; Hoye, T. R.; Mead, C. C.; Kiehl, R. A. *Appl. Phys. Lett.* **2003**, *83*, 5518.
(14) Walzer, K.; Marx, E.; Greenham, N. C.; Less, R. J.; Raithby, P. R.; Stokbro, K. *J. Am. Chem. Soc.* **2004**, *126*, 1229.
(15) Seminario, J. M.; Zacarias, A. G.; Tour, J. M. *J. Am. Chem. Soc.* **2000**, *122*, 3015.
(16) Seminario, J. M.; Zacarias, A. G.; Derosa, P. A. *J. Phys. Chem. A* **2001**, *105*, 791.
(17) Seminario, J. M.; Cordova, L. E.; Derosa, P. A. *Proc. IEEE* **2003**, *91*, 1958.
(18) Taylor, J.; Brandbyge, M.; Stokbro, K. *Phys. Rev. B* **2003**, *68*, 121101.
(19) Stokbro, K.; Brandbyge, M.; Taylor, J.; Ordejón, P. *Ann. N. Y. Acad. Sci.* **2003**, *1006*, 212.
(20) Larade, B.; Taylor, J.; Mehrez, H.; Guo, H. *Phys. Rev. B* **2001**, *64*, 075420.
(21) Seminario, J. M.; Araujo, R. A.; Yan, L. *J. Phys. Chem. B* **2004**, *108*, 6915.
(22) Reed, M. A.; Zhou, C.; Muller, C. J.; Burgin, T. P.; Tour, J. M. *Science* **1997**, *278*, 252.
(23) Stokbro, K.; Taylor, J.; Brandbyge, M.; Mozos, J.-L.; Ordejón, P. *Comput. Mater. Sci.* **2003**, *27*, 151.
(24) Xue, Y.; Ratner, M. A. *Phys. Rev. B* **2003**, *68*, 115406.
(25) Côté, M.; Haynes, P. D.; Molteni, C. *Phys. Rev. B* **2001**, *63*, 125207.
(26) Bai, P.; Yang, S.; Liu, E.; Li, E. *Third IEEE Conf. Nanotechnol. Proc.* **2003**, *2*, 323.
(27) Brandbyge, M.; Mozos, J.-L.; Ordejón, P.; Taylor, J.; Stokbro, K. *Phys. Rev. B* **2002**, *65*, 165401.

Changes of Coupling

J. Phys. Chem. B, Vol. 109, No. 8, 2005 **3339**

(28) Taylor, J.; Guo, H.; Wang, J. *Phys. Rev. B* **2001**, *63*, 245407.

(29) Soler, J. M.; Artacho, E.; Gale, J. D.; Garcia, A.; Junquera, J.; Ordejón P.; Sanchez-Portal, D. *J. Phys.: Condens. Matter* **2002**, *14*, 2745.

(30) Jauho, A.-P.; Wingreen, N. S.; Meir, Y. *Phys. Rev. B* **1994**, *50*, 5528.

(31) Haug, H.; Jauho, A.-P. *Quantum Kinetics in Transport and Optics of Semiconductors*; Springer-Verlag: Berlin, Heidelberg, 1996.

(32) Taylor, J. Ph.D. Thesis, McGill University, 2000.

(33) Wold et al. suggested a value of 2.3 Å for Au−S bond (Wold, D. J.; Haag, R.; Rampi, M. A.; Frisbie, C. D. *J. Phys. Chem. B* **2002**, *106*, 2813), and Sellers et al. suggested 2.011 Å for the Au(100)−S distance at a hollow site (Sellers, H.; Ulman, A.; Shnidman, Y.; Eilers, J. E. *J. Am. Chem. Soc.* **1993**, *115*, 9389.). We adopt a Au−S distance of 2.1 Å as the initial parameter.

(34) Delley, B. *J. Chem. Phys.* **1990**, *92*, 508.

(35) We use a double ζ+polarization basis set for the dithiolborazine molecule and single ζ basis set for the gold s, p, and d channel.

(36) Hamann, D. R.; Schlüter, M.; Chiang, C. *Phys. Rev. Lett.* **1982**, *43*, 1494.

(37) Liang, W.; Shores, M. P.; Bockrath, M.; Long, J.; Park, H. R. *Nature* **2002**, *417*, 725.

(38) Yu, L.; Natelson, D. H. *Nano Lett.* **2004**, *4*, 79.

(39) The changes of coupling intensity can be understood with the following physical picture: the electric field induced by the bias voltage strongly affects the density of states and the orbitals of the molecule near the Fermi level, and this leads to changes of coupling between the molecule and electrodes. Here, the transmission spectra get smaller, which indicates decreasing coupling between the molecule and electrodes.

(40) Roland, C.; Meunier, V.; Larade, B.; Guo, H. *Phys. Rev. B* **2002**, *66*, 035332.

(41) Kaun, C.-C.; Larade, B.; Guo, H. *Phys. Rev. B* **2003**, *67*, 121411-(R).